

Effect of surfactant contamination on a silicone adhesive and adhesive joints with aluminum substrates

CSP Borges (INEGI, Porto, Portugal), R. Brandão, A. Akhavan-Safar, E.A.S. Marques, R.J.C. Carbas, C. Ueffing, P. Weißgraeber, L.F.M. da Silva

Introduction

When contamination is present at the surface of adhesive joints with metallic substrates, it can either **remain at the adhesive/substrate interface** (Figure 1a), resulting in a physical separation between them, or be **absorbed by the adhesive**, changing its properties, particularly at the interphase (Figure 1b).

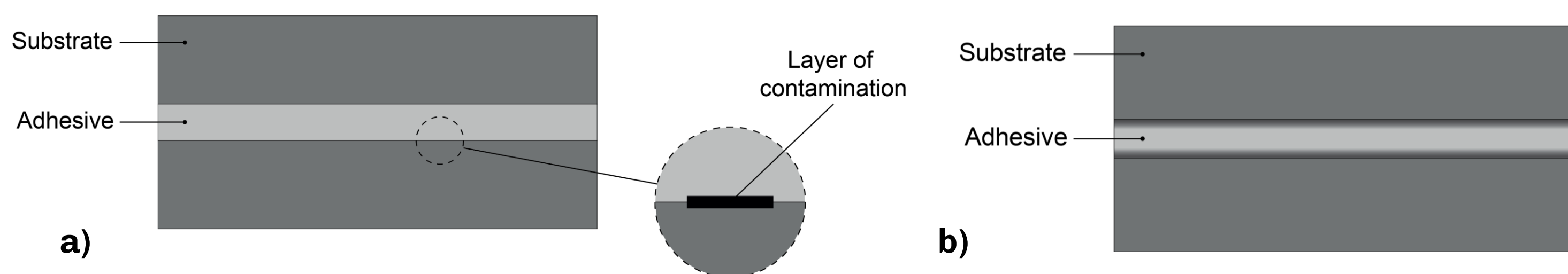


Figure 1 – Contamination and the adhesive/substrate interface a) and contamination absorbed by the adhesive at the interphase b).

The contaminant considered in this work is a **surfactant** used to clean oil off aluminium, after the manufacturing of the component.

Experimental details

Bulk tensile tests, SEM and FTIR analysis were performed using **silicone adhesive with 2%, 5% and 10% of surfactant** mixed into the material prior to curing. Additionally, strength properties of the contaminated joints with **aluminum substrates** and a silicone adhesive were analyzed using single lap joints (SLJ) and the fracture processes using double cantilever beams (DCB).

The substrates were treated with sandpaper and anodized. Afterwards, a **water/surfactant mixture** (with a concentration of 10 g/L) is applied to the substrate, with the contamination levels being established by the **number of sprays deposited**. It is also ensured that **only surfactant is at the substrate prior to bonding** (Figure 2).

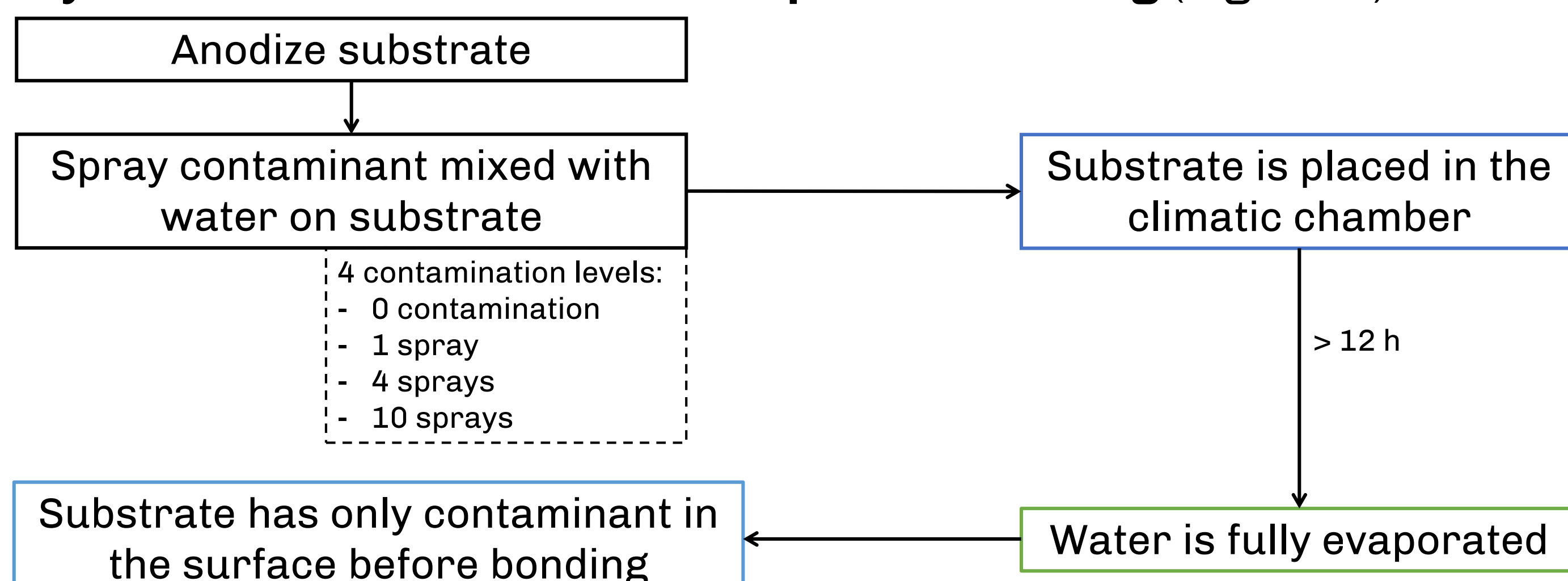


Figure 2 – Substrate treatment procedure prior to bonding.

Experimental results

1. Double cantilever beam (DCB)

Representative **load-displacement curves** obtained from DCB tests for each contamination level are presented in Figure 3.

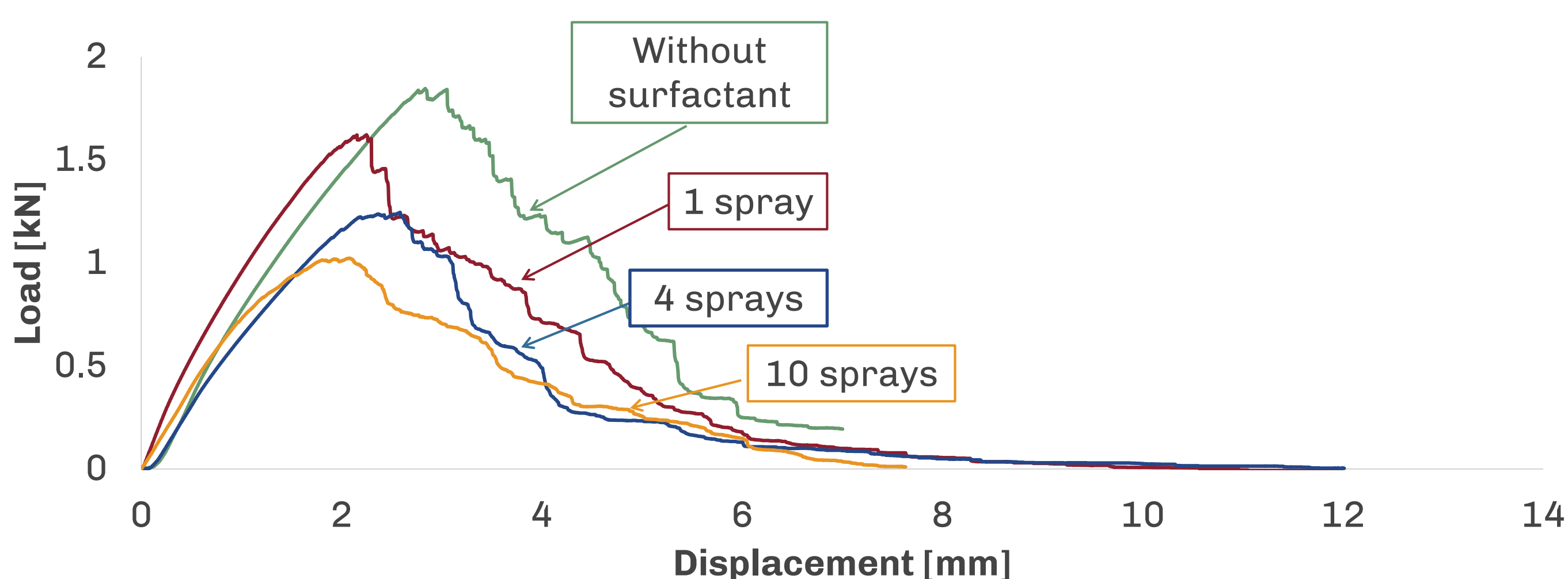


Figure 3 – Representative load-displacement curves for DCB tests for each contamination level

2. Single lap joints (SLJ)

Representative **load-displacement curves** obtained from SLJ tests for each contamination level are presented in Figure 4.

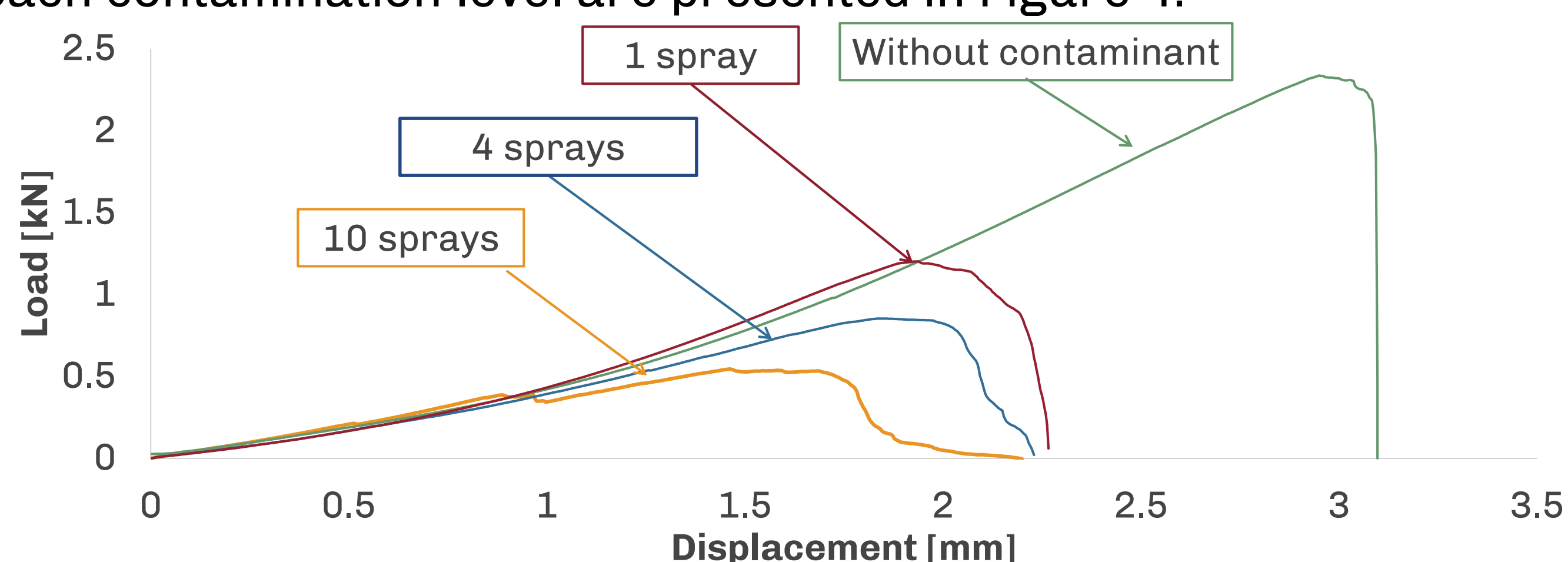


Figure 4 – Representative load-displacement curves for SLJ tests for each contamination level

3. Failure surfaces

The typical **failure surfaces** obtained for each contamination level for DCB and SLJ are shown in Figure 5.

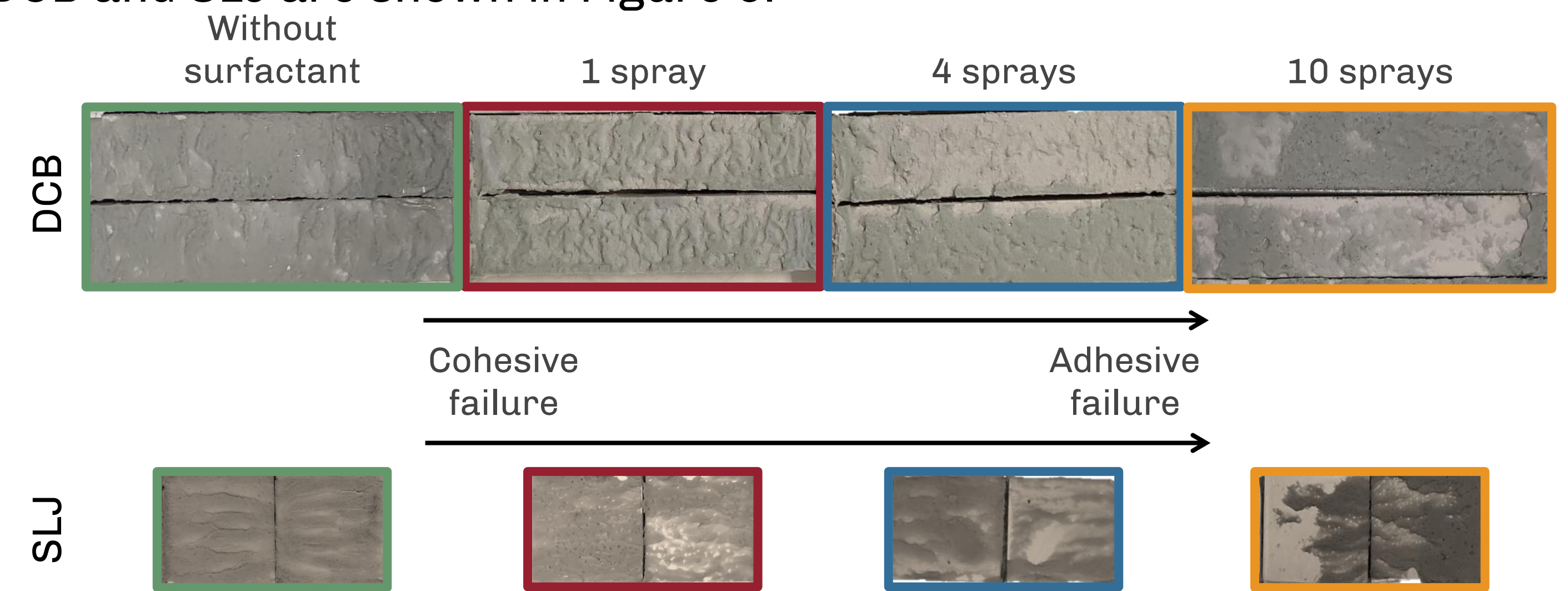


Figure 5 – Fracture surfaces for each contaminant level tested, for SLJ and DCB.

4. Analysis of the bulk adhesive

The results for the **SEM analysis** of the fracture surface of bulk specimens as well as the **FTIR analysis** and **bulk tensile tests** conducted are presented in Figure 6.

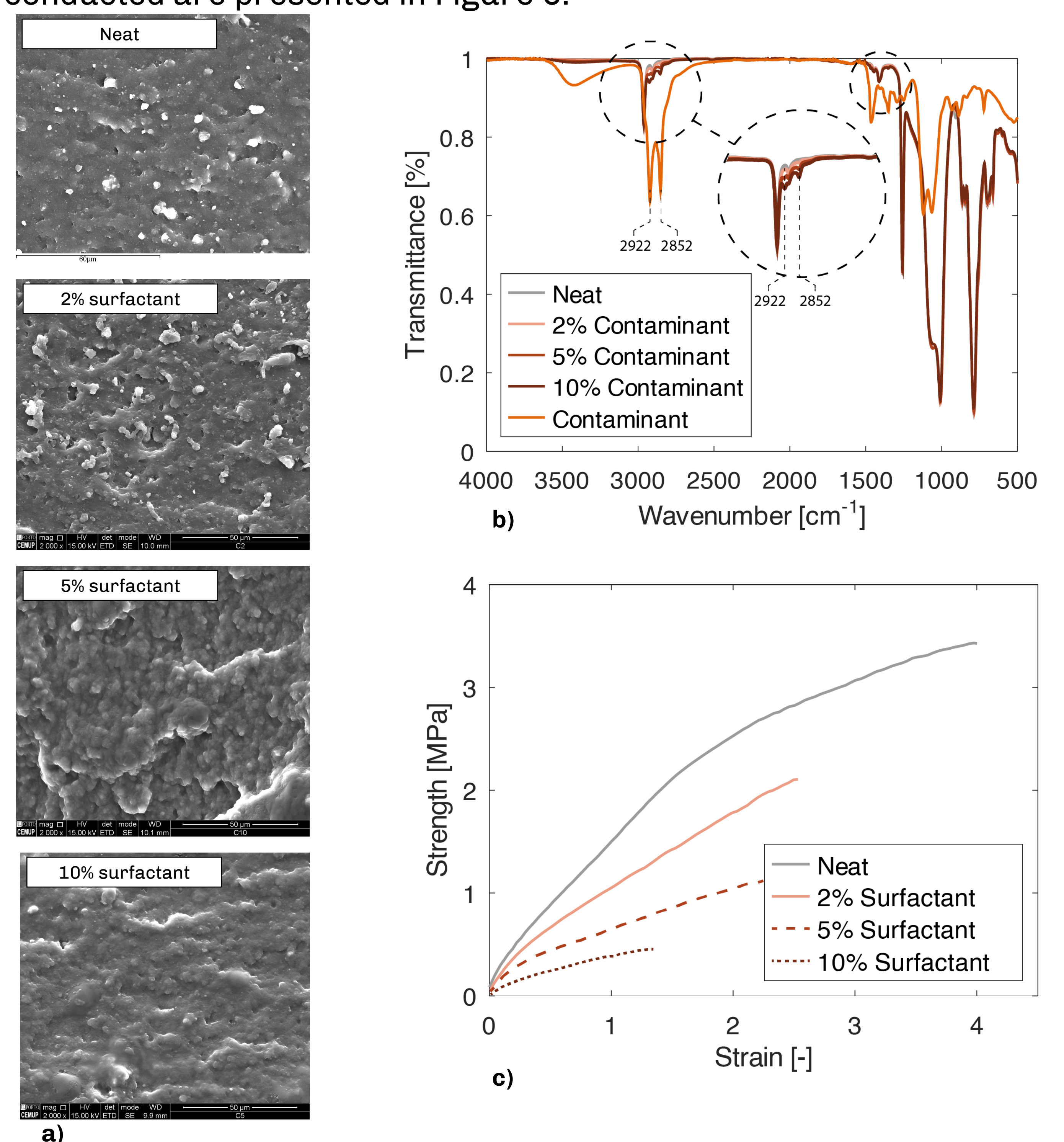


Figure 6 – SEM analysis a), FTIR analysis of the fracture surface b) and bulk tensile test results c).

Conclusions

As the contamination at the surface of the substrate increases, the **failure is progressively interfacial** and the **failure load decreases**. Without contaminant both the DCB and SLJ exhibit cohesive failure, for 1 and 4 sprays of contamination, the **failure path moves closer to the substrate**, as the adhesive near the interface **absorbs contaminant** and weakens its mechanical properties, Figure 1b. As the contamination content increases, the adhesive becomes unable to absorb all the contaminant, leading to **interfacial failure**, Figure 1a.

References

- [1] da Silva L, Öchsner A and Adams R. Handbook of adhesion technology. New York, NY: Springer Science & Business Media, 2018.
- [2] Debski M, Shanahan M and Schultz J. Mechanisms of contaminant elimination by oil-accommodating adhesives Part 1: displacement and absorption. Int J Adhes Adhes 1986; 6: 145–149.
- [3] Borges, C. S. P., Marques, E. A. S., Carbas, R. J. C., Ueffing, C., Weißgraeber, P., & Silva, L. D. (2021). Review on the effect of moisture and contamination on the interfacial properties of adhesive joints. Proceedings of the Institution of Mechanical Engineers, Part C: Journal of Mechanical Engineering Science, 235(3), 527-549.

Acknowledgements

The authors wish to acknowledge and thank the funding and support provided by **Robert Bosch GmbH, Corporate Research and Advance Engineering**. The authors also gratefully acknowledge the funding provided by Fundação para a Ciência e Tecnologia (FCT), Portugal for the Ph.D. Grant 2020.06055.BD.